Solar Phys (2014) 289:4691–4700
DOI 10.1007/s11207-014-0606-7

# Fluence Ordering of Solar Energetic Proton Events Using Cosmogenic Radionuclide Data

**G.A. Kovaltsov · I.G. Usoskin · E.W. Cliver · W.F. Dietrich · A.J. Tylka**

Received: 3 June 2014 / Accepted: 29 September 2014 / Published online: 7 October 2014
© Springer Science+Business Media Dordrecht 2014

**Abstract** While data on the cosmogenic isotopes $^{14}$C and $^{10}$Be made it possible to evaluate extreme solar proton events (SPEs) in the past, their relation to standard parameters quantifying the SPE strengths, *viz.* the integrated fluence of protons with energy above 30 MeV, $F_{30}$, is ambiguous and strongly depends on the assumed shape of the energy spectrum. Here we propose a new index, the integral fluence of an SPE above 200 MeV, $F_{200}$, which is related to the production of the cosmogenic isotopes $^{14}$C and $^{10}$Be in the Earth atmosphere, independently of the assumptions on the energy spectrum of the event. The $F_{200}$ fluence is reconstructed from past cosmogenic isotope data, which provides an assessment of the occurrence probability density function for extreme SPEs. In particular, we evaluate that extreme SPEs with $F_{200} > 10^{10}$ cm$^{-2}$ occur no more frequently than once per 10 – 15 kyr.

**Keywords** Solar energetic particles · Cosmogenic radioisotopes

G.A. Kovaltsov
Ioffe Physical-Technical Institute, St. Petersburg, Russia

I.G. Usoskin (✉)
Sodankylä Geophysical Observatory (Oulu unit), University of Oulu, Oulu, Finland
e-mail: ilya.usoskin@oulu.fi

I.G. Usoskin
Department of Physics, University of Oulu, Oulu, Finland

E.W. Cliver
Space Vehicles Directorate, Air Force Research Laboratory, Kirtland AFB, Albuquerque, NM 87117, USA

E.W. Cliver
National Solar Observatory, Sunspot, NM 88349, USA

W.F. Dietrich
Praxis, Inc., Alexandria, VA 22303, USA

A.J. Tylka
Code 672, NASA Goddard Space Flight Center, Greenbelt, MD 20771, USA

## 1. Introduction

It is of great importance to have a reliable estimate of the flux of solar energetic particles (SEPs) and the probability of occurrence of extreme SEP events (Schrijver *et al.*, 2012). In particular, major SEP events can cause radiation hazards at the level critical for the modern technological community and even potentially affect the Earth climate and biosphere (*e.g.*, Vainio *et al.*, 2009; Atri and Melott, 2014). The era of direct (or indirect) measurements of SEP events is relatively short and spans only several decades, starting with the first detection of a very strong SEP event, *i.e.* an extreme solar proton event (SPE) by ground-based ionization chambers in 1942 (Forbush, 1946). Therefore, the statistics for extreme events are very low and do not provide a solid basis for evaluating the occurrence probability of these events. Moreover, since the modern epoch was characterized by unusually strong and sustained solar activity, the modern Grand Maximum (Solanki *et al.*, 2004), it may not be fully representative of the overall pattern. Therefore, one has to rely on indirect proxy data to reconstruct the history of major SEP events in the past and to evaluate the occurrence probability density function. One such commonly used proxy was nitrate in polar ice, which was proposed to keep a record of major SEP events for several centuries (McCracken *et al.*, 2001; Shea *et al.*, 2006). However, this proxy has been disputed (Wolff *et al.*, 2012), so that nitrates may not serve as a quantitative index of SEP events. Another index used to reconstruct major SEP events in the past is related to records of the cosmogenic radionuclides $^{10}$Be measured in polar ice and $^{14}$C measured in dendrochronologically dated tree rings (Usoskin *et al.*, 2006; Webber, Higbie, and McCracken, 2007). Data on $^{14}$C allow a reliable detection of a possible increase in cosmic rays in 775 AD and 993 AD that is ascribed to extreme SEP events (Miyake *et al.*, 2012; Usoskin and Kovaltsov, 2012; Miyake, Masuda, and Nakamura, 2013a; Usoskin *et al.*, 2013; Jull *et al.*, 2014). However, interpreting these data in terms of the SEP event strength is complicated. A common measure of the SEP event strength is the total fluence of protons with energy above 30 MeV $F_{30}$, or above 10 MeV $F_{10}$. However, cosmogenic isotopes are produced in the Earth atmosphere by more energetic primary particles, above a hundred MeV/nucleon (*e.g.*, Beer, McCracken, and von Steiger, 2012). Therefore the relation between the cosmogenic isotope data and $F_{30}$ (or $F_{10}$) is ambiguous and depends on the assumed SEP energy spectrum (Usoskin and Kovaltsov, 2012; Thomas *et al.*, 2013; Cliver *et al.*, 2014).

Here we focus on determining a parameter of SEP spectra that can be directly assessed from the cosmogenic isotope data without *a priori* assumptions. As reference SEP event spectra we analyze spectra of all the strong SEP events observed by the ground-based network of neutron monitors as ground-level enhancements (GLE – see, *e.g.*, Andriopoulou *et al.*, 2011) for the past 60 years. As the new index of extreme SEP events recorded in the cosmogenic isotope data we propose the event-integrated fluence of protons with energy above 200 MeV, $F_{200}$, which corresponds to a proton rigidity of 645 MV.

## 2. SEP/GLE Event Spectrum

We considered 59 GLE events for the period 1956 – 2012, listed in Table 1, following the approach of Tylka and Dietrich (2009). Energy spectra of protons for the events were reconstructed (Tylka and Dietrich, 2009; Cliver *et al.*, 2014) in the Band functional form, which describes the integral energy spectrum as a double power-law with a smooth exponential roll-over in between. Both the function and its first derivative remain continuous through energy. We express the rigidity $R$ in GV and kinetic energy $E$ in GeV. Then the integral

**Table 1** Dates, official GLE number, and the event-integrated fluence $F_{200}$ (in $cm^{-2}$).

| Date | GLE | $F_{200}$ | Date | GLE | $F_{200}$ |
|---|---|---|---|---|---|
| 1956-Feb-23 | 5 | 1.2E+08 | 1989-Oct-19 | 43 | 5.5E+07 |
| 1959-Jul-17 | 7 | 1.6E+07 | 1989-Oct-22 | 44 | 1.6E+07 |
| 1960-May-04 | 8 | 5.3E+05 | 1989-Oct-24 | 45 | 2.2E+07 |
| 1960-Sep-03 | 9 | 1.5E+06 | 1989-Nov-15 | 46 | 3.2E+05 |
| 1960-Nov-12 | 10 | 6.4E+07 | 1990-May-21 | 47 | 1.4E+06 |
| 1960-Nov-15 | 11 | 3.0E+07 | 1990-May-24 | 48 | 2.4E+06 |
| 1960-Nov-20 | 12 | 1.9E+06 | 1990-May-26 | 49 | 1.6E+06 |
| 1961-Jul-18 | 13 | 6.5E+06 | 1990-May-28 | 50 | 1.0E+06 |
| 1967-Jan-28 | 16 | 4.3E+06 | 1991-Jun-11 | 51 | 4.0E+06 |
| 1968-Nov-18 | 19 | 1.7E+06 | 1991-Jun-15 | 52 | 4.3E+06 |
| 1969-Mar-30 | 21 | 1.7E+06 | 1992-Jun-25 | 53 | 5.4E+05 |
| 1971-Jan-24 | 22 | 3.3E+06 | 1992-Nov-02 | 54 | 2.8E+06 |
| 1971-Sep-01 | 23 | 9.0E+06 | 1997-Nov-06 | 55 | 3.6E+06 |
| 1972-Aug-04 | 24 | 1.4E+07 | 1998-May-02 | 56 | 6.0E+05 |
| 1972-Aug-07 | 25 | 3.1E+06 | 1998-May-06 | 57 | 1.6E+05 |
| 1973-Apr-29 | 26 | 2.3E+05 | 1998-Aug-24 | 58 | 3.9E+05 |
| 1976-Apr-30 | 27 | 7.0E+05 | 2000-Jul-14 | 59 | 3.4E+07 |
| 1977-Sep-19 | 28 | 6.8E+05 | 2001-Apr-15 | 60 | 8.1E+06 |
| 1977-Sep-24 | 29 | 1.4E+06 | 2001-Apr-18 | 61 | 1.2E+06 |
| 1977-Nov-22 | 30 | 2.0E+06 | 2001-Nov-04 | 62 | 1.2E+07 |
| 1978-May-07 | 31 | 4.6E+05 | 2001-Dec-26 | 63 | 1.3E+06 |
| 1978-Sep-23 | 32 | 2.6E+06 | 2002-Aug-24 | 64 | 8.2E+05 |
| 1981-May-10 | 35 | 2.7E+05 | 2003-Oct-28 | 65 | 1.5E+07 |
| 1981-Oct-12 | 36 | 1.4E+06 | 2003-Oct-29 | 66 | 8.2E+06 |
| 1982-Nov-26 | 37 | 4.6E+05 | 2003-Nov-02 | 67 | 1.4E+06 |
| 1982-Dec-08 | 38 | 1.3E+06 | 2005-Jan-17 | 68 | 2.1E+06 |
| 1984-Feb-16 | 39 | 6.9E+05 | 2005-Jan-20 | 69 | 2.2E+07 |
| 1989-Jul-25 | 40 | 4.8E+05 | 2006-Dec-13 | 70 | 5.5E+06 |
| 1989-Aug-16 | 41 | 5.1E+06 | 2012-May-17 | 71 | 1.0E+06 |
| 1989-Sep-29 | 42 | 3.1E+07 | – | – | – |

omnidirectional event-integrated fluence (in protons/$cm^2$) of SEP events can be represented as

$$\begin{aligned} F(>E) &= J_0 \cdot R^{-\gamma_1} \exp\left(-R/R_0\right), \quad \text{for } R \le R_\mathrm{b}, \\ F(>E) &= J_0 \cdot A \cdot R^{-\gamma_2}, \quad \text{for } R > R_\mathrm{b}, \end{aligned} \tag{1}$$

where

$$\begin{aligned} A &= [R_\mathrm{b}]^{(\gamma_2-\gamma_1)} \exp(\gamma_1 - \gamma_2), \\ R &= \sqrt{E^2 + 2E_0 \cdot E}, \end{aligned} \tag{2}$$

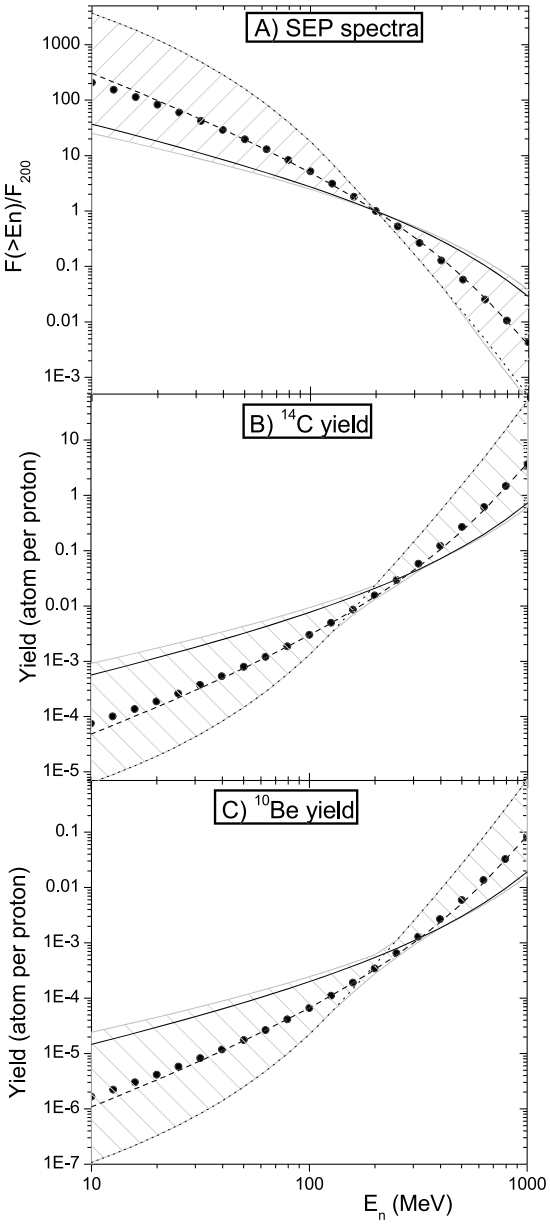


**Figure 1** Yield of cosmogenic isotopes in the 59 GLE events analyzed here as function of the event-integrated fluence of SEPs ($> E_n$). Large dots represent the logarithmic mean value, while the hatched area depicts the full variability range. The solid, dashed, and dotted lines correspond to the GLE5, GLE10, and GLE24 spectra, respectively. A): The ratio of the integral fluence of SEP ($F(> E_n)$) to $F_{200}$, which is normalized to unity. B) and C): Modeled yield curves for $^{14}$C and $^{10}$Be per solar energetic proton with energy above $E_n$.

where $R_b = (\gamma_2 - \gamma_1)R_0$ and $E_0 = 0.938$ GeV is the proton rest-mass energy. Throughout the paper we call $F(> E)$ as $F_E$, where $E$ is expressed in MeV (*e.g.*, $F(> 200$ MeV$) \equiv F_{200}$). We note that the spectral index $\gamma_2$ describes the high-energy tail of the spectrum that we use below to quantify the hardness of the spectrum.

Figure 1A illustrates the range of variability of the integral energy spectrum for the considered GLEs (event-integrated). Spectra for each individual event were normalized by the values of $F_{200}$ for the events (see Table 1). Large solid dots denote the logarithmic mean of

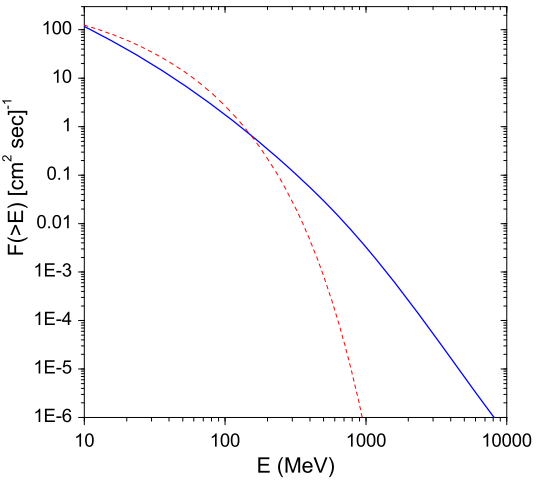


**Figure 2** Integral flux of SEP averaged over the past decades using two different approximations: the all-GLE spectrum used here (blue solid curve, averaged over 1956 – 2012) and the exponent over rigidity spectrum (red dashed curve, averaged over 1954 – 2008, Reedy, 2012).

the spectra, but this mean spectrum is not meaningful because the range of uncertainties at the low and high tails of the spectrum can be as high as a factor of 100 between individual events. We also identified "typical" events for hard, medium and soft spectra. A typical hard-spectrum event is GLE5 (1956-Feb-23, the greatest ever GLE observed by neutron monitors, with the highest enhancement in 1 hr data), a typical medium-soft spectrum event is GLE10 (1960-Nov-12, the second-largest event in $F_{200}$), and a soft-spectrum event is GLE24 (1972-Aug-04, the greatest event in $F_{30}$). The spectra of these typical events are shown as solid, dashed, and dotted lines, respectively, and correspond to the bounds and the mean curve on the plot. Below we compute the production of cosmogenic isotopes for these SEP events.

Here we also compiled the average all-GLE integral SEP spectrum for the last five solar cycles, shown as the blue solid curve in Figure 2. This spectrum includes all the GLE events listed in Table 1 (*viz.* 1956 – 2012). We note that because it includes only GLE events, this spectrum may underestimate the low-energy part where sub-GLE SEP events can contribute to the flux. However, the energy range above 100 MeV is mostly dominated by the GLE event and the sub-GLE event contribution is small, becoming negligible at 200 MeV. Thus, the high-energy tail, based on NM data, is fully representative and corresponds to the observed data.

On the other hand, the integral spectrum of an SEP is often approximated in the form of an exponent-over-rigidity (EOR) function, as proposed by Freier and Webber (1963),

$$F(>E) = F_0 \cdot \exp(-R/R^*). \tag{3}$$

A recent estimate of this for the period 1954 – 2008 ($R^* = 80$ MV, $F(>30$ MeV$) = 35$ protons/cm$^2$/sec) (Reedy, 2012) is shown in Figure 2. We note that these estimates are based only on low-energy space-borne data and apparently heavily underestimate the higher energy range above several hundred MeV (*e.g.*, Mewaldt, 2006), which is important for the cosmogenic isotope production in the atmosphere. Accordingly, we did not use the EOR approximation here because it is inappropriate for the atmospheric cosmogenic isotope production.

## 3. Cosmogenic Isotope Production

### 3.1. Global $^{14}$C Production

For the events analyzed here (Table 1), we calculated the global production of $^{14}$C ($Q_{14C}$) in the Earth atmosphere using a recent model by Kovaltsov, Mishev, and Usoskin (2012). The computed values of $Q_{14C}$ were then normalized for fluences $F_{E_n}$ for each GLE to calculate the yield of the isotope by one solar proton with energy above $E_n$, $Y = Q/F_{E_n}$, as shown in Figure 1B. The plot shows the yield of $^{14}$C (the number of atoms produced in the atmosphere) for one solar proton with energy greater than $E_n$. A cross-cut of this plot is shown in Figure 3 for $E_n = 30$, 200 and 500 MeV, where the $^{14}$C yield is shown as a function of the energy spectrum hardness (parameter $\gamma_2$, see Equation (1)). The spread of the yield is large and systematic for $E_n = 30$ MeV (asterisk symbols). This implies that the relation between $^{14}$C production and the $F_{30}$ fluence is ambiguous up to a factor of 40 and strongly depends on the spectral shape so that it is greater for soft spectra and smaller for hard spectra. The use of a too high $E_n = 500$ MeV also leads to a large spread with an oppositely skewed relation. If the energy $E_n$ is chosen correctly, however, *viz.* 200 MeV, the relation is unambiguous within $\pm 30$ % and is almost independent of the spectral shape. It can be seen in Figure 1B as a narrowing of the variability ranges with increasing $E_n$ until approximately 200 MeV. After that, the range starts to increase.

This implies that $F_{200}$ is directly linked to the SEP-related atmospheric production of $^{14}$C. The relation is such that $(1.6 \pm 0.2) \times 10^{-2}$ atoms of globally averaged $^{14}$C are produced per $F_{200}$ fluence. The radiocarbon response to an SEP event can be unambiguously converted into the $F_{200}$ fluence, but this leads to large uncertainties for the $F_{30}$ fluence. The values of $F_{200}$ for the strongest events of 775 AD and 993 AD are $\approx 8 \times 10^9$ and $6 \times 10^9$ cm$^{-2}$. Such extreme SEP fluences may lead to an underestimate of the $^{14}$C-based sunspot number reconstruction for these decades that were found to be small $\approx 20-30$ (Usoskin *et al.*, 2014; Cliver *et al.*, 2014). A proper account for this leads to higher sunspot numbers of $50-60$, but this is still about 30 % lower than that of Solar Cycle 19 (Bazilevskaya *et al.*, 2014).

For the famous Carrington event (Cliver and Dietrich, 2013), the values of $F_{200}$ can be evaluated as follows: Annual $^{14}$C data (Stuiver *et al.*, 1998; Miyake, Masuda, and Nakamura, 2013b) for that period depict that there is no $\Delta^{14}$C increase greater than 2 per mille (measurement errors), leading to a conservative limit of $F_{200} \leq 10^9$ cm$^{-2}$.

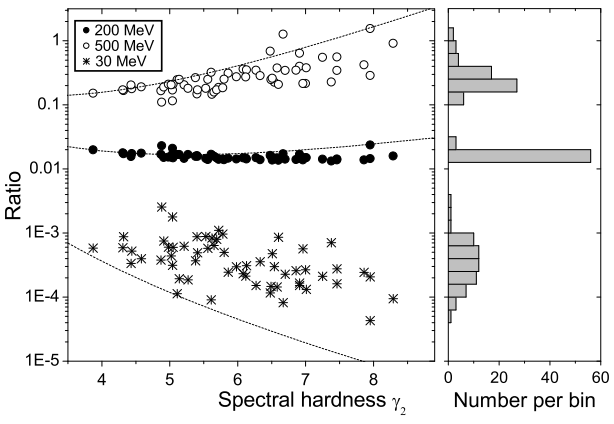


**Figure 3** The yield of $^{14}$C atmospheric production by SEPs as a function of the hardness of the high-energy tail of the spectrum quantified through the spectral parameter $\gamma_2$ (Equation (1)) for the modern geomagnetic field and three values of $E_n = 30$, 200, and 500 MeV, as indicated in the legend. Symbols correspond to the actual GLE events, while lines depict the theoretically expected ratio assuming a pure power-law spectrum. The right-hand panel depicts the distribution histograms of the values.

### 3.2. $^{10}$Be Deposition in Polar Ice

Similar to the radiocarbon isotope $^{14}$C above, we studied the relation between the SEP event-integrated fluence and the deposition of $^{10}$Be isotope in polar ice. Using the SEP energy spectra discussed here and a recent model of the $^{10}$Be yield (Kovaltsov and Usoskin, 2010), we have calculated the production of $^{10}$Be in a 3D realistic atmosphere (see a description of the method in Usoskin *et al.*, 2009). For the beryllium transport and deposition we considered the medium model by Usoskin *et al.* (2009), with the polar tropospheric and hemispherically mixed stratospheric productions (Vonmoos, Beer, and Muscheler, 2006; McCracken, 2004). The corresponding yield of $^{10}$Be deposited in polar ice is shown in Figure 1C. Similarly as for $^{14}$C, the relation between $F_{E_n}$ and $^{10}$Be is optimal at $E_n \approx 200$ MeV, where the uncertainty is smallest and independent of the spectral shape. This generally agrees with the effective energy of the $^{10}$Be production (see Figure 6 in Webber, Higbie, and McCracken, 2007). The yield of $^{10}$Be deposited in polar ice per the unit fluence $F_{200}$ is $(3.4 \pm 0.5) \times 10^{-4}$ in the framework of the adopted transport model.

In contrast, because of the much harder spectrum of Galactic cosmic rays, their production of cosmogenic nuclei is sensitive to higher energies (Usoskin, 2013) and is ordered by $F_{2500}$ for $^{14}$C and $F_{2000}$ for $^{10}$Be.

## 4. Reconstruction of $F_{200}$ in the Past

Using these computations for the $^{14}$C and $^{10}$Be, we recalculated all the candidates of extreme SEP events in the past several millennia (for the Holocene) into the optimum fluence $F_{200}$. The events were taken from Table 1 of Usoskin and Kovaltsov (2012), with the 775 AD event revised according to Miyake *et al.* (2012) and Usoskin *et al.* (2013) and a new recently discovered event of 993 AD (Miyake, Masuda, and Nakamura, 2013a) added. The new integral occurrence probability density function of the annual values of $F_{200}$ is presented in Figure 4a. It is quite different from the earlier one (Schrijver *et al.*, 2012; Usoskin and Kovaltsov, 2012), which was built for $F_{30}$ assuming a hard SEP spectrum (as for the event of 1956-Feb-23), but it also implies a strong roll-over of the events with an extreme fluence (Figure 4b). The estimated value of $F_{30}$ is ambiguous and depends on the assumption of the unknown spectrum of SPE, as indicated by the red arrow in the Figure. We note, however, that the data based on lunar rocks favor a hard spectrum (Kovaltsov and Usoskin, 2014). The $F_{200}$ does not have this uncertainty.

We note that $F_{200}$ values for the events in the high-fluence branch are higher by 10 – 50 times than the values for the strongest recent cycle (No. 19; 1954 – 1964) during the Modern Grand Maximum. This may be related to a detection threshold due to the weak sensitivity of the cosmogenic isotopes to low-energy CR particles (Beer, McCracken, and von Steiger, 2012; Usoskin, 2013) and a low temporal resolution of one year at best. Thus, the SEP events should be strong enough to produce at least 10 % of the radionuclide compared with the annual production by galactic cosmic rays. This sets an effective detection threshold of $F_{200} > 2 \times 10^9$ cm$^{-2}$ and the corresponding occurrence probability of once per several centuries (the left upper open star-point in Figure 4a). The right-most open-circle point corresponds to the largest detected events, *viz.* 775 AD. Moreover, we are sure from decadal data that no events with $F_{200} > 10^{10}$ cm$^{-2}$ took place during the Holocene (see details in Usoskin and Kovaltsov, 2012), which sets an upper limit (the right-most black dot) on the occurrence probability for such an event as once per 10 – 15 kyr. An essential steepening of the distribution between low- and high-fluence events is apparent, which qualitatively agrees

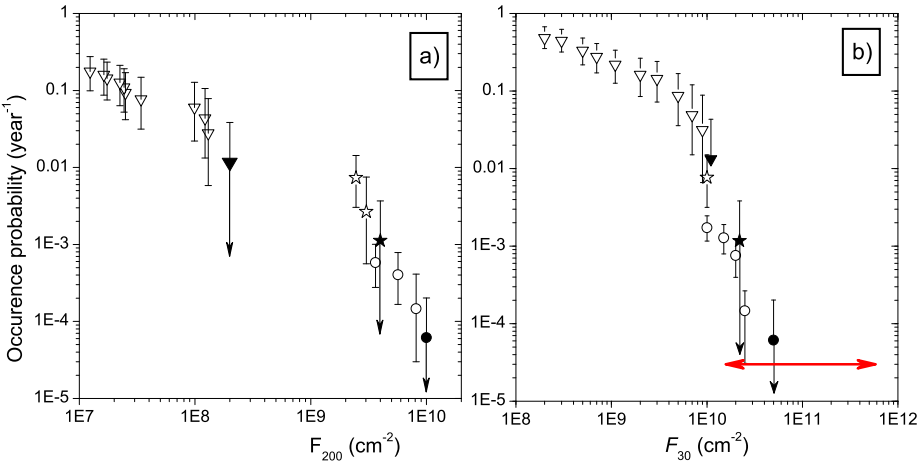


**Figure 4** The cumulative occurrence probability density function of annual fluences greater than the given value on the X-axis. Panel (a) is for the $F_{200}$ obtained here. Panel (b) is for the $F_{30}$ (modified after Figure 5 of Usoskin and Kovaltsov, 2012): symbols are for the assumption of a hard SPE spectrum, while the range of uncertainty due to the unknown spectral shape is indicated by the red arrow. Points correspond to the annual fluences for the space era, since 1955 (triangles) and cosmogenic radionuclides in terrestrial archives for the Holocene: high-resolution (annual) data for several centennia (stars), and low-resolution data for millennia (circles). Open symbols correspond to the statistics of "observed" data, while filled symbols denote the conservative upper limit (no events greater than X observed during Y years). Error bars correspond to the 90 % confidence level evaluated assuming Poisson statistics.

with many earlier studies based on $F_{10}$ or $F_{30}$ (*e.g.*, Smart and Shea, 2002; Schrijver *et al.*, 2012).

The absence of data points from the modern era with annual $F_{200}$ values $> 1.2 \times 10^8$ cm$^{-2}$ (corresponding to 1956-Feb-23) is puzzling because the Modern Grand Maximum (1945 – 1995) is the most active interval of the past few millennia (Usoskin, 2013; Cliver *et al.*, 2014). We note that while we used only GLE data in this plot, including sub-GLE events (*i.e.*, observable proton increases above 300 MeV that did not register in neutron monitors, see Tylka and Dietrich in preparation) does not affect the statistics of these high-fluence events. There are other more exotic hypotheses for the high-fluence historical events observed in $^{14}$C and $^{10}$Be, such as galactic gamma-bursts (Pavlov *et al.*, 2013, see also references in Cliver *et al.*, 2014 for other non-solar alternatives). Strictly speaking, it cannot be excluded that the gap in Figure 4 separates two distributions – solar on the left and galactic gamma-burst on the right. On the other hand, this distribution provides the conservative upper limit for the SEP fluence.

## 5. Conclusions

We have shown that the integral fluence of strong SPE events above 200 MeV, $F_{200}$, is related to the production of the cosmogenic isotopes $^{14}$C and $^{10}$Be in the Earth atmosphere, independently of the assumptions on the event energy spectrum. Thus, the $F_{200}$ fluence can be reconstructed from the cosmogenic isotope data in the past, in contrast to fluence $F_{30}$, whose uncertainty in this type of reconstruction can be as large as a factor of 40. In Figure 4 we presented the occurrence probability density function for extreme SEP events as

compiled from data for the modern epoch high-resolution and low-resolution cosmogenic isotope data. In particular, we evaluated that extreme SEP events with an $F_{200}$ fluence greater than $10^{10}$ cm$^{-2}$ occur no more frequently than once per 10 – 15 kyr.

**Acknowledgements** G.A. Kovaltsov is grateful to the Academy of Finland for partial support. I.G. Usoskin's contribution was made in the framework of the ReSoLVE Centre of Excellence (Academy of Finland, project no. 272157). E.W. Cliver acknowledges support from the Air Force Office of Scientific Research. A.J. Tylka and W.F. Dietrich are supported by NASA Solar & Heliophysics SR&T under NNH12AT09I.

## References

Andriopoulou, M., Mavromichalaki, H., Plainaki, C., Belov, A., Eroshenko, E.: 2011, Intense ground-level enhancements of solar cosmic rays during the last solar cycles. *Solar Phys.* **269**, 155. DOI.

Atri, D., Melott, A.L.: 2014, Cosmic rays and terrestrial life: a brief review. *Astropart. Phys.* **53**, 186. DOI.

Bazilevskaya, G.A., Cliver, E.W., Kovaltsov, G.A., Ling, A.G., Shea, M., Smart, D., Usoskin, I.G.: 2014, Solar cycle in the heliosphere and cosmic rays. *Space Sci. Rev.*, in press. DOI

Beer, J., McCracken, K., von Steiger, R.: 2012, *Cosmogenic Radionuclides: Theory and Applications in the Terrestrial and Space Environments*, Springer, Berlin.

Cliver, E.W., Dietrich, W.F.: 2013, The 1859 space weather event revisited: limits of extreme activity. *J. Space Weather Space Clim.* **3**(26), A31. DOI.

Cliver, E.W., Tylka, A.J., Dietrich, W.F., Ling, A.G.: 2014, On a solar origin for the cosmogenic nuclide event of 775 A.D. *Astrophys. J.* **781**, 32. DOI.

Forbush, S.E.: 1946, Three unusual cosmic-ray increases possibly due to charged particles from the Sun. *Phys. Rev.* **70**, 771. DOI.

Freier, P.S., Webber, W.R.: 1963, Exponential rigidity spectrums for solar-flare cosmic rays. *J. Geophys. Res.* **68**, 1605. DOI.

Jull, A.J.T., Panyushkina, I.P., Lange, T.E., Kukarskih, V.V., Myglan, V.S., Clark, K.J., Salzer, M.W., Burr, G.S., Leavitt, S.W.: 2014, Excursions in the $^{14}$C record at ad 774 – 775 in tree rings from Russia and America. *Geophys. Res. Lett.* **41**, 3004. DOI.

Kovaltsov, G.A., Mishev, A., Usoskin, I.G.: 2012, A new model of cosmogenic production of radiocarbon $^{14}$C in the atmosphere. *Earth Planet. Sci. Lett.* **337**, 114.

Kovaltsov, G.A., Usoskin, I.G.: 2010, A new 3D numerical model of cosmogenic nuclide $^{10}$Be production in the atmosphere. *Earth Planet. Sci. Lett.* **291**, 182. DOI.

Kovaltsov, G.A., Usoskin, I.G.: 2014, Occurrence probability of large solar energetic particle events: assessment from data on cosmogenic radionuclides in lunar rocks. *Solar Phys.* **289**, 211. DOI.

McCracken, K.G.: 2004, Geomagnetic and atmospheric effects upon the cosmogenic $^{10}$Be observed in polar ice. *J. Geophys. Res.* **109**(A18), A04101. DOI.

McCracken, K.G., Dreschhoff, G.A.M., Zeller, E.J., Smart, D.F., Shea, M.A.: 2001, Solar cosmic ray events for the period 1561 – 1994: 1. Identification in polar ice, 1561 – 1950. *J. Geophys. Res.* **106**, 21585.

Mewaldt, R.A.: 2006, Solar energetic particle composition, energy spectra, and space weather. *Space Sci. Rev.* **124**, 303. DOI.

Miyake, F., Masuda, K., Nakamura, T.: 2013a, Another rapid event in the carbon-14 content of tree rings. *Nat. Commun.* **4**, 1748. DOI.

Miyake, F., Masuda, K., Nakamura, T.: 2013b, Lengths of Schwabe cycles in the seventh and eighth centuries indicated by precise measurement of carbon-14 content in tree rings. *J. Geophys. Res.* **118**, 7483. DOI.

Miyake, F., Nagaya, K., Masuda, K., Nakamura, T.: 2012, A signature of cosmic-ray increase in ad 774 – 775 from tree rings in Japan. *Nature* **486**, 240. DOI.

Pavlov, A.K., Blinov, A.V., Konstantinov, A.N., Ostryakov, V.M., Vasilyev, G.I., Vdovina, M.A., Volkov, P.A.: 2013, AD 775 pulse of cosmogenic radionuclides production as imprint of a Galactic gamma-ray burst. *Mon. Not. Roy. Astron. Soc.* **435**, 2878. DOI.

Reedy, R.C.: 2012, *Update on Solar-Proton Fluxes During the Last Five Solar Activity Cycles*, *Lunar and Planetary Institute Science Conference Abstracts* **43**, Springer, Berlin, 1285.

Schrijver, C.J., Beer, J., Baltensperger, U., Cliver, E.W., Güdel, M., Hudson, H.S., McCracken, K.G., Osten, R.A., Peter, T., Soderblom, D.R., Usoskin, I.G., Wolff, E.W.: 2012, Estimating the frequency of extremely energetic solar events, based on solar, stellar, lunar, and terrestrial records. *J. Geophys. Res.* **117**, A08103. DOI.

Shea, M.A., Smart, D.F., McCracken, K.G., Dreschhoff, G.A.M., Spence, H.E.: 2006, Solar proton events for 450 years: the Carrington event in perspective. *Adv. Space Res.* **38**, 232.

Smart, D.F., Shea, M.A.: 2002, A review of solar proton events during the 22nd solar cycle. *Adv. Space Res.* **30**, 1033.

Solanki, S.K., Usoskin, I.G., Kromer, B., Schüssler, M., Beer, J.: 2004, Unusual activity of the Sun during recent decades compared to the previous 11 000 years. *Nature* **431**, 1084. DOI.

Stuiver, M., Reimer, P.J., Bard, E., Burr, G.S., Hughen, K.A., Kromer, B., McCormac, G., van der Plicht, J., Spurk, M.: 1998, Intcal98 radiocarbon age calibration, 24 000-0 cal BP. *Radiocarbon* **40**(3), 1041.

Thomas, B.C., Melott, A.L., Arkenberg, K.R., Snyder, B.R.: 2013, Terrestrial effects of possible astrophysical sources of an AD 774 – 775 increase in $^{14}$C production. *Geophys. Res. Lett.* **40**, 1237. DOI.

Tylka, A., Dietrich, W.: 2009, A new and comprehensive analysis of proton spectra in ground-level encahnced (GLE) solar particle events. In: *31th International Cosmic Ray Conference*, Universal Academy Press, Lodź.

Usoskin, I.G.: 2013, A history of solar activity over millennia. *Living Rev. Solar Phys.* **10**, 1. DOI.

Usoskin, I.G., Kovaltsov, G.A.: 2012, Occurrence of extreme solar particle events: assessment from historical proxy data. *Astrophys. J.* **757**, 92. DOI.

Usoskin, I.G., Horiuchi, K., Solanki, S., Kovaltsov, G.A., Bard, E.: 2009, On the common solar signal in different cosmogenic isotope data sets. *J. Geophys. Res.* **114**, A03112. DOI.

Usoskin, I.G., Kromer, B., Ludlow, F., Beer, J., Friedrich, M., Kovaltsov, G.A., Solanki, S.K., Wacker, L.: 2013, The AD775 cosmic event revisited: the Sun is to blame. *Astron. Astrophys.* **552**, L3. DOI.

Usoskin, I.G., Hulot, G., Gallet, Y., Roth, R., Licht, A., Joos, F., Kovaltsov, G.A., Thébault, E., Khokhlov, A.: 2014, Evidence for distinct modes of solar activity. *Astron. Astrophys.* **562**, L10. DOI.

Usoskin, I.G., Solanki, S.K., Kovaltsov, G.A., Beer, J., Kromer, B.: 2006, Solar proton events in cosmogenic isotope data. *Geophys. Res. Lett.* **33**, L08107. DOI.

Vainio, R., Desorgher, L., Heynderickx, D., Storini, M., Flückiger, E., Horne, R.B., Kovaltsov, G.A., Kudela, K., Laurenza, M., McKenna-Lawlor, S., Rothkaehl, H., Usoskin, I.G.: 2009, Dynamics of the Earth's particle radiation environment. *Space Sci. Rev.* **147**, 187. DOI.

Vonmoos, M., Beer, J., Muscheler, R.: 2006, Large variations in holocene solar activity: constraints from $^{10}$Be in the Greenland ice core project. *J. Geophys. Res.* **111**(A10), A10105. DOI.

Webber, W.R., Higbie, P.R., McCracken, K.G.: 2007, Production of the cosmogenic isotopes $^{3}$H, $^{7}$Be, $^{10}$Be, and $^{36}$Cl in the Earth's atmosphere by solar and galactic cosmic rays. *J. Geophys. Res.* **112**, A10106. DOI.

Wolff, E.W., Bigler, M., Curran, M.A.J., Dibb, J.E., Frey, M.M., Legrand, M., McConnell, J.R.: 2012, The Carrington event not observed in most ice core nitrate records. *Geophys. Res. Lett.* **39**, L08503. DOI.